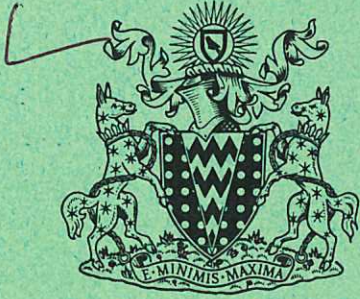


This document is intended for publication in a journal, and is made available on the understanding that extracts or references will not be published prior to publication of the original, without the consent of the authors.

CULHAM LABORATORY
LIBRARY
21 NOV 1972



UKAEA RESEARCH GROUP

Preprint

THE CLEO TOKAMAK NEUTRAL INJECTION SYSTEM

D ALDCROFT
J BURCHAM
H C COLE
M COWLIN
J SHEFFIELD

CULHAM LABORATORY
Abingdon Berkshire

1972

PL 1-100

PL 1-100
PL 1-100
PL 1-100
PL 1-100
PL 1-100

Enquiries about copyright and reproduction should be addressed to the Librarian, UKAEA, Culham Laboratory, Abingdon, Berkshire, England

THE CLEO TOKAMAK NEUTRAL INJECTION SYSTEM

D. Aldcroft, J. Burcham, H.C. Cole, M. Cowlin and J. Sheffield.

(Submitted for publication in Nuclear Fusion)

ABSTRACT

An intense beam of neutral hydrogen atoms will be injected into the plasma of the CLEO Tokamak. This beam will be used to provide additional heating of the plasma and for a general investigation of the beam-plasma interaction. It is estimated that a 60kW beam, of 50 msec duration at 30keV will raise the plasma temperature by typically 10%. A neutral injection system which meets this minimum requirement is described.

UKAEA Research Group,
Culham Laboratory,
Abingdon,
Berkshire
June 1972.

1. INTRODUCTION

The use of an intense beam of neutral atoms to raise the temperature of the plasma on a fusion reactor to ignition is currently of great interest⁽²⁾⁽⁸⁾⁽¹³⁾. There are, however, a number of uncertainties in the technique which must be resolved. In particular; the effect of a build up of space charge due to charge separation following ionization of the fast neutrals by the plasma; the possibility of instabilities occurring; the effect of imparting angular momentum to the plasma; all require experimental investigation. The importance of the injection system described below is that it provides a means of investigating both the plasma heating and the effects which are by-products of the interaction.

A schematic diagram of the CLEO Tokamak, showing the two injection lines is shown in Figure 1. The beams are injected close to the tangent to the major toroidal circumference. The fast neutrals are first ionised on the background plasma and then share their energy by collisions with this plasma. The fast ions are born with their velocity primarily parallel to B_{ϕ} , the

toroidal magnetic field, and the majority of them are on contained orbits. It is calculated in section 5 that the incremental temperature rise produced by a single 60 kW (70 per cent at 30 keV, 30 per cent at 15 keV), 50 msec duration neutral beam will be $\frac{\Delta T_i}{T_{i0}} \sim 0.1 \rightarrow 0.3$ $\frac{\Delta T_e}{T_{e0}} \sim 0.05 \rightarrow 0.08$. This is on the limit of detector capability, and a second line of inferior access, but which offers an additional 30 kWatts of neutral power, will be added later.

The main parameters of the Tokamak are major radius $R = 90$ cm minor radius of plasma $a = 18$ cm, axial field $B_\phi = 20$ kGauss maximum, axial current $I_\phi = 90$ kA maximum. Scaling from other Tokamak results, in particular the T-3⁽¹⁾ suggest the plasma parameters will be typically, average density $n \sim 2 \times 10^{13} \text{ cm}^{-3}$, average electron temperature $T_e \sim 300$ eV, average ion temperature $T_i \sim 200$ eV.

2. INJECTION SYSTEM

This paper reports the results of an extensive series of tests made with the Mark I (5 cm electrode diameter) multiaperture ion source (121 apertures). The tests were made in a vacuum chamber 25 cm diameter, 133 cm long and also on the complete injection system. The results, particularly the good beam divergence, encouraged us to increase the size of the electrodes to 7.5 cm diameter (235 apertures) and it is this Mark II source which is shown in the drawing of the final injection system, (see Figure 2).

The results of the tests on the two sources are summarized in Table 1. The performance is comparable with that reported by O.R.N.L.⁽²⁾, on whose work our design was based.

MK I Source

MK II Source

	Unbowed electrodes 6.1mm main gap	Bowed electrodes 4.1mm main gap	Bowed electrodes 4.1mm main gap
Accelerator voltage kV	37.5	31.5	25
Univalent Beam Current Amp	2.7	3.1	> 5
Total beam power kW	100	100	>125
Neutral power into LEO kW	35	45	60

TABLE 1. SOURCE PERFORMANCE

Plasma Source:- A hydrogen plasma is produced by an ORNL duopigatron arc source⁽²⁾. This plasma illuminates a 7.5 cm diameter multiaperture three electrode system, (Figure 3). The electrode nearest the plasma is at the positive potential V_A . This can be varied from 10 to 36 keV. The centre electrode is held at the negative potential $V_D = -\frac{V_A}{8}$. The third electrode is at earth potential.

The plasma ions at the plasma-vacuum interface are accelerated through the electrodes and we end up with an ion beam of energy V_A (eV).

Neutraliser:- The ion beam is neutralised by background hydrogen gas in the first chamber. For our beam energies we require a target thickness of 0.15 Torr cm to approach equilibrium. This is achieved using gas from the source by restricting the pumping close to the electrodes with a 20 cm length of tube. The gas pressure in the body of the chamber is typically 2×10^{-3} Torr.

The source is tested and the electrodes conditioned by firing the beam onto the calorimeters in the neutraliser chamber. In this mode the gas is removed from the system entirely by the diffusion pump. For injection into CLEO the central 8 cm diameter

calorimeter is retracted.

Differential Pumping:- Between the neutraliser and the torus is a second chamber which contains a titanium getter system; this is water cooled and has an area of about 1000 cm². This chamber is isolated from the torus by a gate valve and from the neutraliser by a fast shutter. The measured gas flow into CLEO is reduced to around 1 amp equivalent by this differential pumping system. The latter also serves the purpose of reducing the gas pressure in the region of strong B_θ field so that the fast neutrals are not ionized and deflected out of the beam

Charged particle deflector and dump:- The charged particles remaining in the beam after neutralisation are deflected sideways by the B_φ field in the region of the gate valve. When the gate valve is opened a 9 cm diameter titanium tube is pushed through it towards the torus. This tube collects the deflected charged particles ⁽³⁾ and it also protects the gate valve. When the titanium tube is retracted it may be degassed by heating.

Fast shutter:- In the retracted position the titanium tube makes a vacuum seal to the fast shutter and prevents it being moved. Thus for injection into CLEO we open the gate valve, push the titanium tube through and then operate the fast shutter. The time for one complete operation of this shutter is 0.7 sec, with 0.2 sec fully open.

3. TEST RESULTS ON MARK I ION SOURCE (Figure 4)

Source Parameters:- The maximum flow of H₂⁰ is about 1 Torr litre sec⁻¹ (5 Amps equivalent). The plasma is formed by an arc which is struck between a hollow copper anode and an oxide coated filament. The arc voltage is 150 V the current of order 50 A; this is supplied by an 160 mF electrolytic capacitor bank. The pulse duration is normally 50 msec.

The plasma profile and density is adjusted by varying the magnetic fields of the compressor and the auxiliary coil. The

beam power is critically affected by the level of the magnetic fields, and on the Mark II source we have made provision to adjust the axial position of the auxiliary coil so that we can determine the effect it has on the extraction region. Our main concern is with the effect of the radial component of this field on the ion trajectories. The plasma illuminates a 5 cm diameter three electrode accel-decel system, (see Figure 3). The electrodes have 121 accurately aligned apertures of radii respectively $r_1 = 1.85$ mm, $r_2 = r_3 = 1.4$ mm. The plasma electrode transparency is 67 per cent. The gap separations for work up to 32 keV are $d_1 = 4.1$ mm and $d_2 = 1.5$ mm. This geometry was based upon the work of Thompson and Coupland⁽⁴⁾ and Coupland et al⁽⁵⁾. For operation at higher voltages (40 keV) the first gap was set at $d_1 = 6.1$ mm.

The positive potential V_A is supplied by a 100 μ F capacitor bank. The negative potential is steady state. The source magnet supplies and the filament are pulsed on for 12 seconds, starting at 10 seconds prior to the application of V_A . The gas is pulsed on shortly before the arc voltage is applied; this latter is switched on 20 msec after V_A .

Ion Beam:- The source produces a beam of mixed ions of energy V_A (eV). The total energy in the pulse was measured using a copper calorimeter of known mass with a thermocouple to monitor the temperature rise. The pulse duration τ and an indication of the temporal behaviour of the beam was obtained from the electrical current to the calorimeter. The average equivalent current I_B is defined as $I_B = \frac{W}{V_A \tau}$. This current is plotted against V_A in Figure 5 for $d_1 = 4.1$ mm and $d_1 = 6.1$ mm. Both curves are fitted by a current which follows the voltage dependence of the plane diode formula⁽⁵⁾.

$$I_B = N\mu(V_A + |V_D|)^{\frac{3}{2}} \quad \dots(1)$$

N is the number of apertures.

The perveance per aperture has the approximate form

$$\mu \approx c \pi \frac{r^2}{d_1^2} \quad \dots(2)$$

The measured average value of the constant c for 121 apertures consistent with the results of Figure 4 is

$$c = 0.7 \pm 0.1 \times 10^{-8} \text{ Amp(V)}^{-\frac{3}{2}} \text{ per aperture} \quad \dots(3).$$

This is to be compared with the theoretical plane diode limit for which

$$\mu_{\max} = 7.3 \times 10^{-6} \frac{r^2}{d_1^2} \left(\frac{m_e}{m_i} \right)^{\frac{1}{2}}$$

and which yields for our case

$$c_{\max} = 5 \times 10^{-8} \text{ Amp(V)}^{-\frac{3}{2}} \text{ per aperture} \quad \dots(4).$$

The difference between \bar{c} and c_{\max} occurs partly because the 121 apertures were not uniformly illuminated, and in addition corrections to the plane diode formula which allow for the real geometry lead to a lower theoretical value for c_{\max} . This we know because in tests on a single aperture system of similar geometry Coupland et al⁽⁵⁾ have obtained

$$c = 3.7 \times 10^{-8} \text{ Amp(V)}^{-\frac{3}{2}} \text{ per aperture} \quad \dots(5)$$

Beam divergence:- The beam profile was measured in a test chamber. All the beam was collected by the four concentric calorimeters, diameters 9.1, 12.6, 15.6 and 25.6 cm respectively, set at 133 cm from the source. The smoothed beam profile in current density is plotted in Figure 6. 85 per cent of the beam is within a 12.6cm diameter; this corresponds to a half angle of divergence of 1.6° . The divergence angle is defined here as the increase in the beam diameter over 133 cm. This low divergence, bearing in mind that there is no focussing magnet, is achieved in part by curving the positive $\sim 0.5\text{mm}$ deflection at the centre and negative $\sim 0.2\text{mm}$ deflection at the centre electrodes towards the plasma source and in part by rapid neutralization of the beam as it leaves the source. The background pressure of hydrogen gas was always kept

above 0.5×10^{-3} Torr for these measurements. The result is particularly encouraging because it shows that the single aperture divergence found by Coupland et al⁽⁵⁾ may be extended to multiaperture systems.

Efficiency of Beam Production:- The positive current drain, the negative current drain and the total equivalent beam current were all measured. We found that within 5 per cent

$$|I_+| = |I_-| + |I_B| \quad \dots(6)$$

and that $|I_-| \lesssim 3\%(I_+)$ under reasonable operation conditions. Thus the source is better than 97% efficient in extraction. The peak power extracted was 100 kW, the power dissipated in producing the plasma was ≤ 10 kW, therefore the overall electrical efficiency is greater than 90%.

Neutralisation efficiency and beam content:- The charged component remaining in the beam after it had been neutralised was analysed with a deflection magnet and Faraday Cup. Three main peaks were observed and these occurred at magnetic fields in the ratio 2:1.4:1. The components were therefore H_2^+ at V_A , H_1^+ at V_A and H_1^+ at $\frac{V_A}{2}$. The latter component comes from dissociation of H_2^+ . The peak electrical currents to the Faraday cup were in the ratio 0.1:1.2:0.3 respectively. The measurements were made at $V_A = 25$ keV with a chamber 150 cm long and a mean background pressure of 10^{-3} Torr. The level of H_2^+ suggests that 90% of this component had been dissociated which indicates that the system was close to the equilibrium state. The neutralization cross section per hydrogen atom at 25 keV is $2.5 \times 10^{-16} \text{ cm}^2$, the equilibrium fraction of neutrals is 0.76, at 12.5 keV the figures are $4 \times 10^{-16} \text{ cm}^2$ and 0.88, (see Stier and Barnett⁽⁶⁾). It can be shown by working back from these results that the neutral beam energy was invested in approximately 70% of H_1^0 at 25 keV and 30% of H_1^0 at 12.5 keV. The total beam power was measured calorimetrically with and without a deflection magnetic field strong enough to deflect all the charges. The neutralization fraction was 0.7.

Gas efficiency:- the measured peak flow rate of H_2^0 was 0.6 Torr litre sec^{-1} (3.4 A equivalent). This was obtained by measuring the volume of hydrogen at atmospheric pressure expelled by the vacuum pumps in a fixed period of time. The peak beam current was 3.1 A (75% H_1^+ , 25% H_2^+). The equivalent current of H_2^+ was therefore $I_+ = 1.9$ A and the gas efficiency is therefore 55%.

Electrode Damage:- The results described here were all taken with the same set of copper electrodes. These electrodes have withstood more than 2,000 pulses of 50 msec duration at beam currents in the region of 2A with no observable damage. Pulses up to 150 msec duration at over 1 Amp have also been obtained. Attempts with similar electrodes to run either DC or for times of order one second have also resulted in distortion/melting of the central area of the positive electrode. This electrode heating problem is discussed by Cole et al⁽⁷⁾. Among the conclusions of this paper is that molybdenum would be better able to withstand the thermal loading. We have in fact successfully used molybdenum electrodes for 50 msec pulses. Two final points of interest:

- (1) When the beam is extracted, the electrodes get hot and expand. A flat electrode structure then has three options; it can bow either towards or away from the plasma or it can buckle. One cannot risk the latter alternative, therefore it is sensible to start with a slightly curved electrode convex towards the plasma. This also reduces beam divergence.
- (2) It is necessary to fire a large number of pulses (~100) in order to condition the electrodes so that they can withstand the full extraction voltage. Electrodes which have finally operated at 30 kV would not initially hold off 15 kV. This may be due to the evolution of gas, or to dirt on the surfaces (though the electrodes were electro-polished) or to the removal of loose bits

of metal from the surface.

4. TEST RESULTS ON MARK II SOURCE (Figure 7)

The complete injection system has undergone preliminary tests with the Mark II source (7.5 cm electrodes, 235 apertures, $r_1 = 1.85$ mm, $r_2 = r_3 = 1.4$ mm, $d_1 = 4.1$ mm, $d_2 = 1.5$ mm).

The total power at a given extraction voltage is double that of the MK I source, thus the extracted power per unit area of electrodes is the same. The peak current to date exceeds 5A equivalent at $V_A = 25$ keV.

The optimum electrode curvature is now being determined. Over focussing was obtained when the deflection of the centre of the plasma electrode was 2.5 mm. A deflection of 0.5mm gave good focussing.

The gas flow at these high currents was 1 Torr litre sec^{-1} (5.6A) of H_2^0 . In the absence of the beam the current to the diffusion pump in the neutraliser chamber was 3.1 A, and that through the injection line with no getter 2.5A. With the titanium getter working the latter flow was reduced to about 1 A equivalent.

5. INTERACTION OF THE NEUTRAL BEAM WITH THE PLASMA

There are three stages to this calculation:-

- (a) we calculate the amount of the neutral beam which is trapped in the plasma,
- (b) we determine the percentage of the trapped power which is transferred to the plasma, and estimate how this power is shared between the electrons and ions.
- (3) We estimate the change in ion and electron temperatures which is caused by this additional heating.

The calculations are based on the work of Sweetman⁽⁸⁾, Stix⁽⁹⁾ and Gibson⁽¹⁰⁾.

The following parameters are used.

Total injected neutral power $P_{NT} = 60$ kW duration 50 msec
(70% of the power is at 30 keV, 30% at 15 keV).

Initial electron temperature $T_e = 300$ eV, ion temperature
 $T_i = 200$ eV, density $n = 2 \times 10^{13} \text{ cm}^{-3}$.

Axial magnetic field $B_\omega = 20$ kG. Axial current $I_\omega = 80$ kA.

Major radius $R_0 = 90$ cm, minor radius of plasma $a = 18$ cm.

Ionisation of beam:- The penetration depth for $1/e$ attenuation of a neutral beam of energy $\epsilon_i \geq 15$ keV is given by (8)

$$\ell = \frac{5 \times 10^{10} \epsilon_i (\text{eV})}{n (\text{cm}^{-3})} \text{ cm} \quad \dots (7)$$

This is not very dependent on the plasma temperature because the collisions are primarily charge exchange for 15 keV.

We are injecting close to the tangent to major circumference and obviously we want to have $\ell < L_c = 2(2R_0 a)^{1/2}$ the chord length. For our conditions $\ell \approx 40 \rightarrow 80$ cm $< L_c \approx 112$ cm. Thus we expect essentially all of the neutral beam to be converted to fast ions.

Contained orbits:- The fast ions start with their velocity primarily in the direction of the magnetic field and they follow orbits, the projections of which on a radial plane are approximately circles. The circles are centered on a point which is displaced along the major radius away from the toroidal magnetic axis, (see Fig. 8).

For parallel injection, i.e., in the direction of the Joule heating current, the displacement is towards the central axis of the torus; for anti-parallel injection it is away from the central axis. Near the magnetic axis the displacement is

$$\Delta \approx \pm \frac{a}{R_0} \rho_{i\theta} \quad \text{where} \quad \rho_{i\theta} = 140 \frac{[\epsilon_i (\text{eV})]^{1/2}}{B_\theta (\text{Gauss})} \text{ cm}$$

is the gyroradius of an

injected ion in the poloidal field, B_θ , where this is taken at $r = a$. For CLEO $B_\theta = 1.0$ kG and for $\epsilon_i = 30$ keV, $\rho_{i\theta} = 24$ cm
 $\Delta = \pm 4.8$ cm.

Parallel injection:- For ions created close to the median plane, all orbits are contained when the creation point is within the limits $R = R_0 - (a-\Delta)$ to $R_0 = a$, or in our case $R = 77$ to 108 cm. From Figure 9, we see that 60% of the neutrals are on trajectories which keep them in the safe region, and there is a high probability that the other 40% will be ionised before they reach the unsafe region. We therefore estimate that 90% of the 15 keV component will be born on contained orbits and 80% of the 30 keV component.

Anti-parallel injection:- In this case because the drift centre is displaced inwards, the ions created on the outside of the plasma i.e. with $R > R_0 + (a-\Delta) = 103$ cm are lost immediately to the limiter. Fortunately Δ is small and in the outer regions the density is very low and again most of the fast ions will be contained, about 80% of each component.

Power Transfer to the Plasma

For $\epsilon > \epsilon_{cr} \simeq 16 T_e$ (eV) for protons on a hydrogen plasma (8) (9) the rate of transfer of energy to the plasma electrons exceeds that to the ions. For $\epsilon < \epsilon_{cr}$ the reverse is true.

Significant angular scattering does not occur until the fast ions have slowed to an energy at which they interact primarily with the plasma ions. Therefore we do not expect the fast ions to deflect into an untrapped orbit until $\epsilon < \epsilon_{cr}$, and most probably not until $\epsilon \sim T_i$, which in comparison to ϵ_i is essentially zero. Stix⁽⁹⁾ has estimated the division of energy between the electrons and ions for classical collisions for the case where the fast ion transfers all of its energy.

For our case $\epsilon_{cr} = 5$ keV and if G_e and G_i are the fractions of the incident power going to the electrons and ions respectively,

we find for $\epsilon_i = 30$ keV ($G_e = 0.73$ $G_i = 0.27$)

$\epsilon_i = 15$ keV ($G_e = 0.55$ $G_i = 0.45$)

For $P_{NT} = 60$ kW (70% at 30 keV and 30% at 15 keV) these figures combine to give $P_{Ne} = 34$ kW $P_{Ni} = 16$ kW.

Effect of Neutrals in the Plasma

There are two significant sources of neutrals in the body of the plasma:-

1. Plasma ions charge exchange with neutral atoms at the wall; these plasma temperature neutrals have a long free path and can reach the centre of the plasma. Measurements on the T-3 Tokamak (11) (12) indicate that neutral densities from this source can reach $1 \rightarrow 5 \times 10^8 \text{ cm}^{-3} = n_{n1}$.

2. Neutrals are left behind when the fast neutral beam is trapped. The neutral density from this source is

$$n_{n2} \approx \frac{I_B \tau}{1.6 \times 10^{-19}} \text{ cm}^{-3} \quad (8)$$

where I_B is the neutral beam current in amps, V is the plasma volume $2 \times 10^5 \text{ cm}^3$ and τ is the containment time for these neutrals. Both the transit time across a diameter of the torus and the ionisation time are about 10^{-6} sec.

With $I_B = 3A$ we obtain $n_{n2} = 10^8 \text{ cm}^{-3}$.

We will assume that in total $n_n \leq 5 \times 10^8 \text{ cm}^{-3}$.

The neutralisation rate for $1 \text{ keV} < \epsilon < 30 \text{ keV}$ is approximately constant at $1.5 \times 10^{-7} \text{ cm}^3 \text{ sec}^{-1}$. The mean free time for neutralisation is

$$\tau_N = \frac{1}{n_n \times 1.5 \times 10^{-7}} = 13 \text{ msec} \quad \dots (9)$$

The time for an ion to slow down from ϵ_i to $0(T_i)$ is (8,9)

$$\tau_s \approx 3 \times 10^{-3} \ln \left[1 + \frac{\epsilon_i}{\epsilon_r} \right] \text{ sec} \quad \text{for CLEO conditions.}$$

For both species $\tau_s < \tau_N$ and we should therefore not experience problems with these slow neutrals. Note that even when an ion is reneutralised it will probably be ionised again before it leaves the plasma, thus one

neutralising collision is not disastrous.

Heating by the Neutral Beam

In the absence of additional heating by neutral injection we have at constant temperature (T_0) a balance between the power loss from a species $P_L(T_0)$ and the power input $P_J(T_0)$ (Joule heating for electrons, electron-ion collisions for ions)

$$P_L(T_0) - P_J(T_0) = 0 \quad \dots(10)$$

With neutral injection the temperature of each species changes to T_s .

$$P_{Ls}(T_s) - P_{Js}(T_s) = P_{Ns} \quad \dots(11)$$

We set

$$\begin{aligned} P_{Ls} &= a_s T_s^{\alpha_s} &) \\ P_{Js} &= b_s T_s^{\beta_s} &) \end{aligned} \quad \dots(12)$$

i.e., we assume that the two power balance equations may be decoupled, and find that the final temperature is given by

$$P_{Ns} = v_s T_0^{\beta_s} \left[\left(\frac{T_s}{T_{0s}} \right)^{\alpha_s} - \left(\frac{T_s}{T_{0s}} \right)^{\beta_s} \right] \quad \dots(13)$$

or

$$\frac{\Delta T_s}{T_{0s}} \approx \frac{P_{Ns}}{(\alpha_s - \beta_s) b_s T_{0s}^{\beta_s}}$$

Heating of the electrons:-

The Joule heating of the electrons is given by^(8,9,10)

$$P_{Je} = 0.16 \Psi \frac{R}{a} \frac{I^2}{a} [T_e(\text{eV})]^{-\frac{3}{2}} \text{ Watts} \quad \dots(14)$$

where the factor Ψ allows for the anomalous nature of the resistivity. For the T-3 tokamak conditions⁽¹⁾ $\Psi \approx 3$, and we take this as a sensible correction factor. For $I = 8 \times 10^4 \text{ A}$

$$R/a = 5 \quad a = 18 \text{ cm}$$

$$b_e = 0.85 \times 10^9 \text{ Watts (eV)}^{1.5} \quad \text{and} \quad \beta_i = -1.5.$$

If the loss rate has a neo-classical dependence on temperature then we have

$$P_{Le} \propto T_e^{1/2} \quad \text{and} \quad \alpha_e = 0.5$$

If the loss has a Bohm type of dependence on T_e $\alpha_e = 2$.
 With $P_{Ne} = 34$ kW we find

$\frac{\Delta T_e}{T_{eo}} \Rightarrow 0.06 \text{ to } 0.10$ <p style="text-align: center;">Bohm neo-classical</p>
--

Heating of the ions:- The ions are heated by collisions with the electrons and

$$P_{Ji} \approx 0.76 \times 10^{-27} \left[\frac{T_e - T_i}{T_e^{3/2}} \right] n^2 \ln \Lambda \text{ Watts cm}^{-3} \quad \dots (15)$$

T_e, T_i in eV.

For $\frac{T_e}{T_i}$ in the range 1.6 to 8 the factor in square brackets (1) becomes $(0.34 \pm 0.04) T_i^{-1/2}$ it is independent of T_e which is consistent with our decoupling of the power balance equations. We are close enough to this regime $\left(\frac{T_{eo}}{T_{io}} \sim 1.5 \right)$ and the incremental temperature rise is small enough for us to use this approximation. For a parabolic density distribution at a peak density $n = 2 \times 10^{13} \text{ cm}^{-3}$ we obtain

$$P_{Ji} = 4.2 \times 10^5 T_i^{-1/2} \text{ Watts}$$

Thus $b_i = 4.2 \times 10^5 \text{ Watts (eV)}^{1/2}$ and $\beta_i = -0.5$

In the banana regime $\alpha_i = 0.5$

In the plateau regime $\alpha_i = 2.5$.

With $P_{Ni} = 16$ kW $T_{io} = 200$ eV we find

$\frac{\Delta T_i}{T_{io}} \Rightarrow 0.12 \text{ to } 0.36$ <p style="text-align: center;">plateau banana</p>
--

From a neo-classical point of view the ions will be in the banana regime as long as

$$\left(\frac{a}{R}\right)^{\frac{3}{2}} \gg \frac{qR}{\lambda_{ii}} \approx \frac{2R}{\lambda_{ii}} \quad \text{or} \quad \lambda_{ii} \gg 2 \times 10^3 \text{ cm}$$

$$\lambda_{ii} \approx \frac{2.2 \times 10^{13} [T_i (\text{eV})]^2}{n (\text{cm}^{-3}) \ln \Lambda} \quad \text{for} \quad T_{i0} = 200 \text{ eV} \quad \lambda_{ii} = 3 \times 10^3 \text{ cm}$$

The result is not clear cut and one must therefore assume the worst and we see in total that for 60 kW neutral input the incremental temperature rise will be of order 10%. This is on the limit of our detector capability and we have therefore incorporated a second injection line to raise the injected neutral power. This second line has a small final aperture but it should be possible to inject at about half the level of the first line i.e., 30 kW.

ACKNOWLEDGEMENTS

The authors are pleased to have the opportunity of acknowledging the help of Dr. O. B. Morgan of ORNL. The calculations of heating effects are based upon the work of Drs. D. R. Sweetman and A. Gibson with whom the authors have had many valuable discussions.

REFERENCES

1. Artsimovich, L.A., Glukhov, A.V., Petrov, M.P. JETP Letts. 1970, 11, 304
and
Gorbunov, E.P., Mirnov, S.V., Strelkov, V. Nuclear Fusion 1970, 10, 43.
2. Davis, R.C., Morgan, O.B., Stewart, L.D., Stirling, W.L. Rev.Sci.Inst. 1972, 43, 278.
3. McCracken, G.M., Jeffries, D.K., Goldsmith, P., Proc. of IVth Int. Vacuum Congress, 1968, 149.
4. Coupland, J.R., Thompson, E. 1970, CLM P-251.
5. Coupland, J., Green, T., Hammond, P., Riviere, A.C. 1972 CLM P-312.
6. Stier, P.M., Barnett, C.F., Phys.Rev. 1956, 103, 896.
7. Cole H.C., Hammond D.P., Riviere A.C., Sheffield, J. 1972, CLM P-313.
8. Sweetman, D. 1972, CLM P-311.
9. Stix, T.H. Plasma Physics 1972, 14, 1.
10. Gibson, A. Private communication.
11. Isaenko, L.F., Macorov, L.V., Shcheglov D.A., JETP Letts. 1970, 12, 217.
12. Peacock, N.J., Robinson, D.C., Culham Report CLM-R107, 1970.
13. Sweetman, D.R., Riviere, A.C., Cole, H.C., Thompson, E., Hammond, D.P., Hugill, J., McCracken, G.M., (1971). Fourth Conference on Plasma Physics and Controlled Nuclear Fusion Research. I.A.E.A. Madison, Wisconsin, CN-28/K-5.

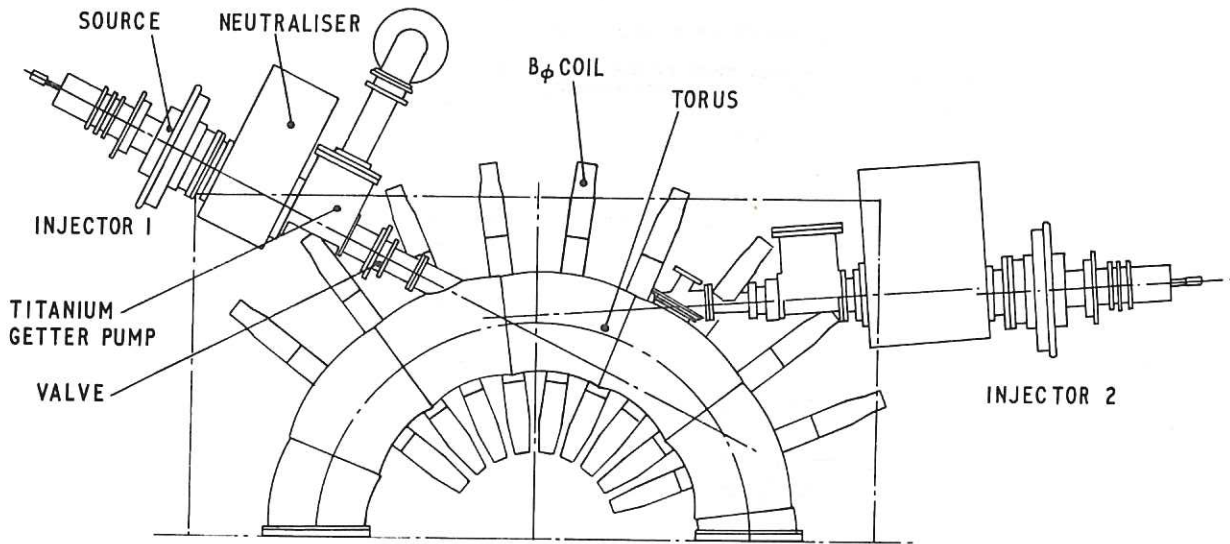


Fig.1 A section of the CLEO torus and two injection systems

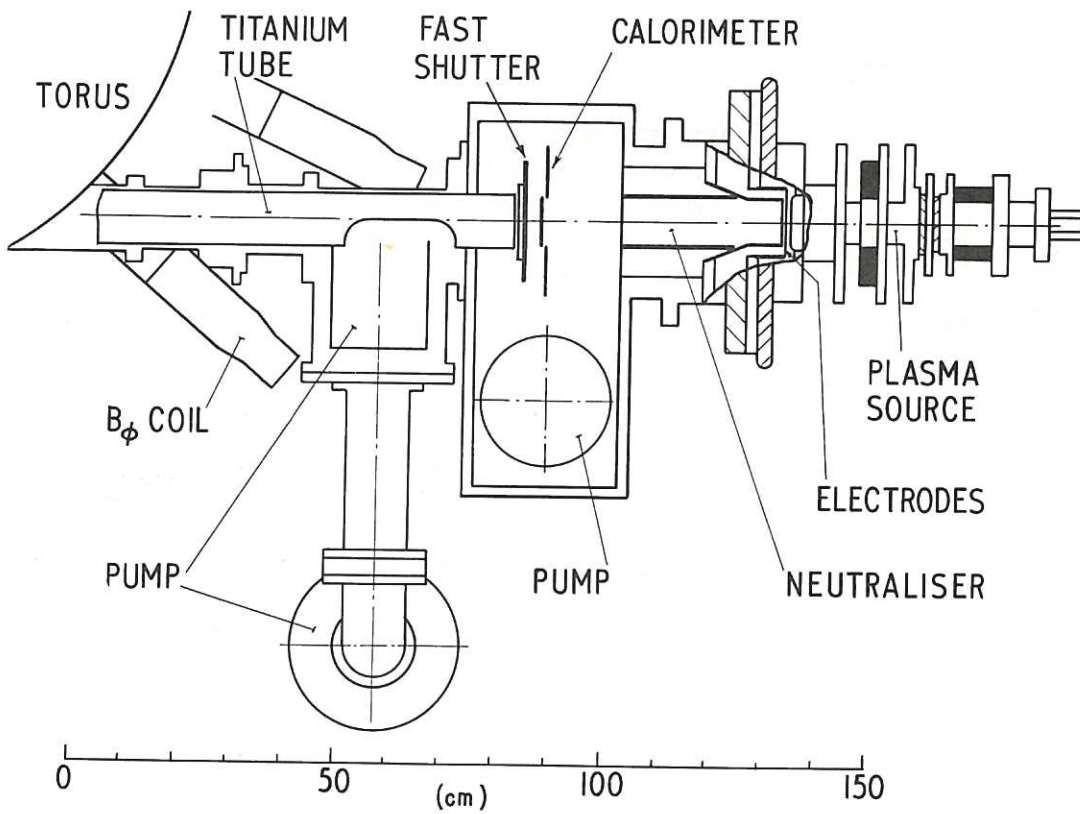


Fig.2 A neutral injection system

CLM-P314

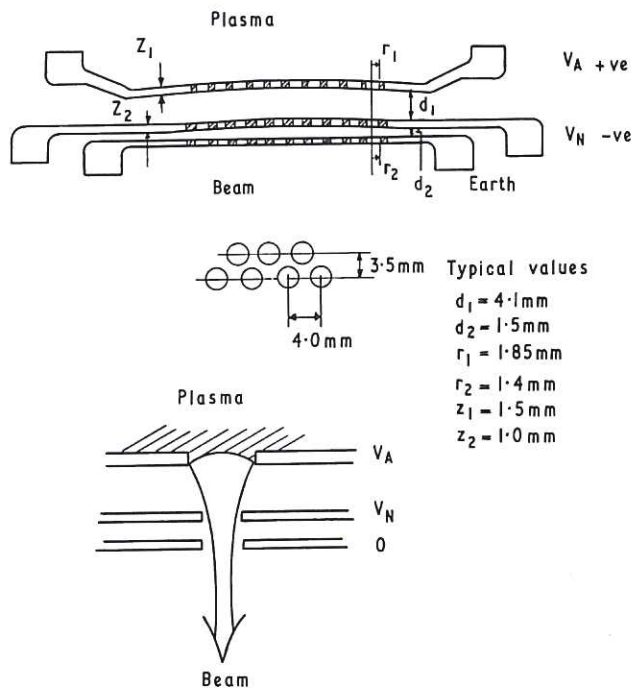


Fig. 3 Extraction geometry

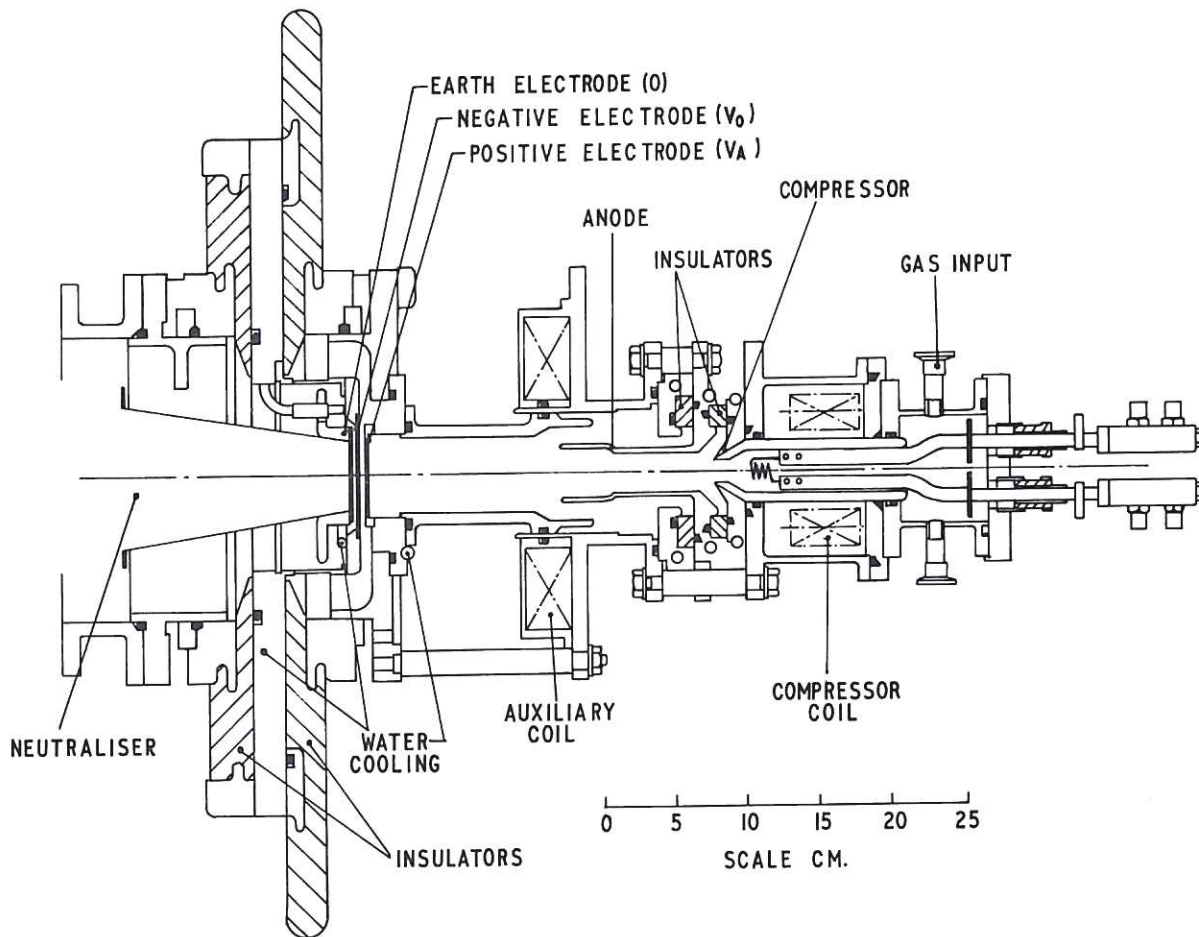


Fig. 4 The Mk I multiaperture ion source

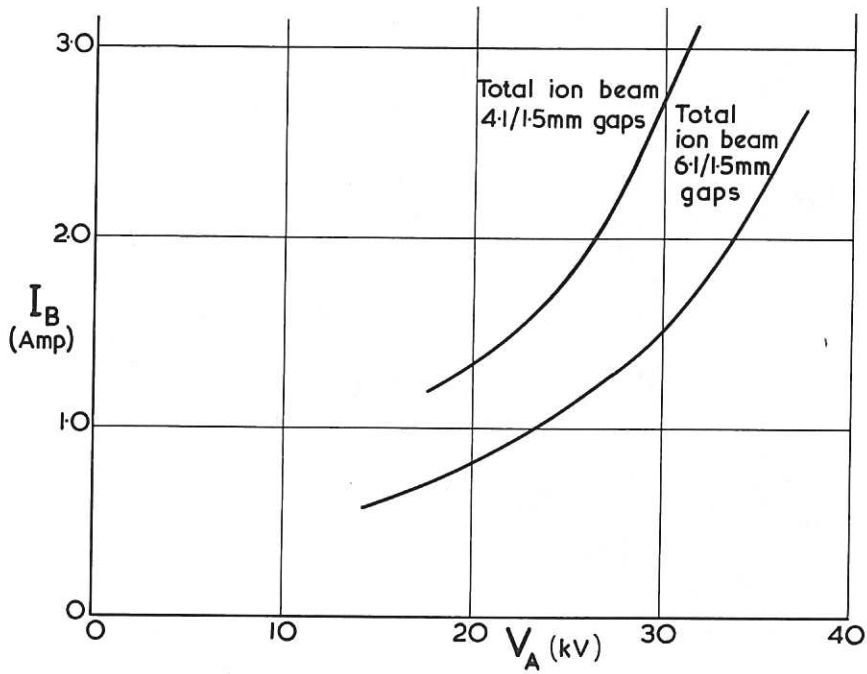


Fig. 5 The equivalent ion beam current for the Mk I source as a function of the acceleration voltage

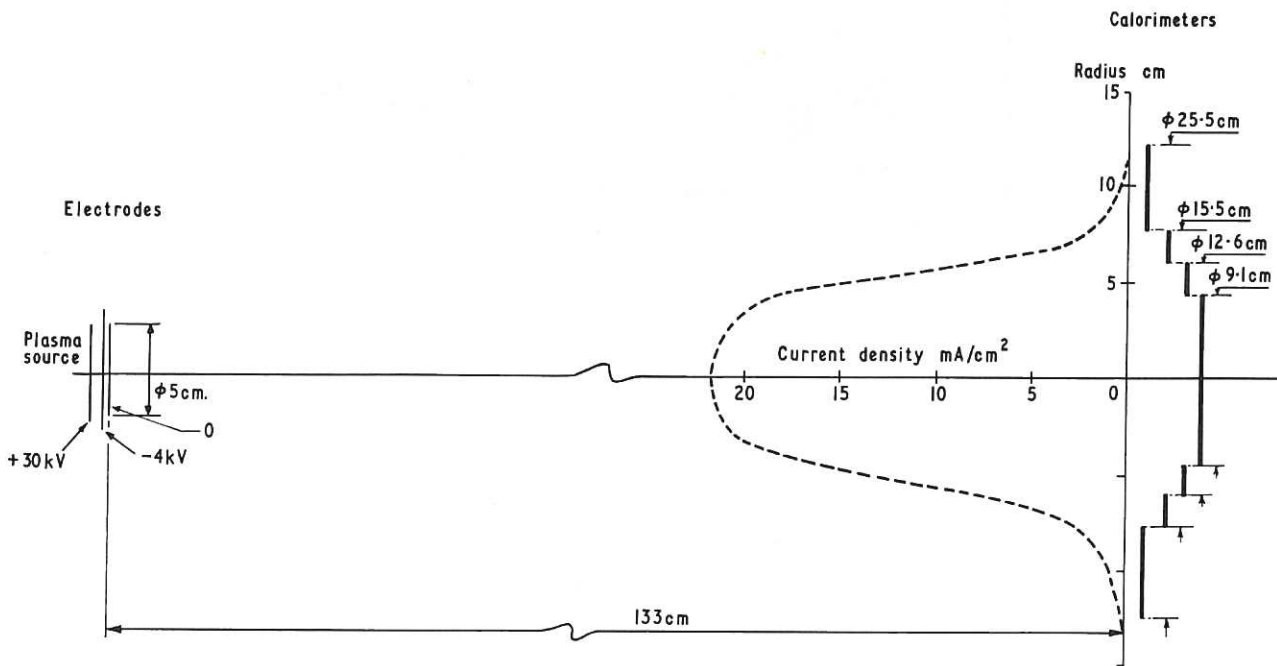


Fig. 6 The beam current density profile for the Mk I source

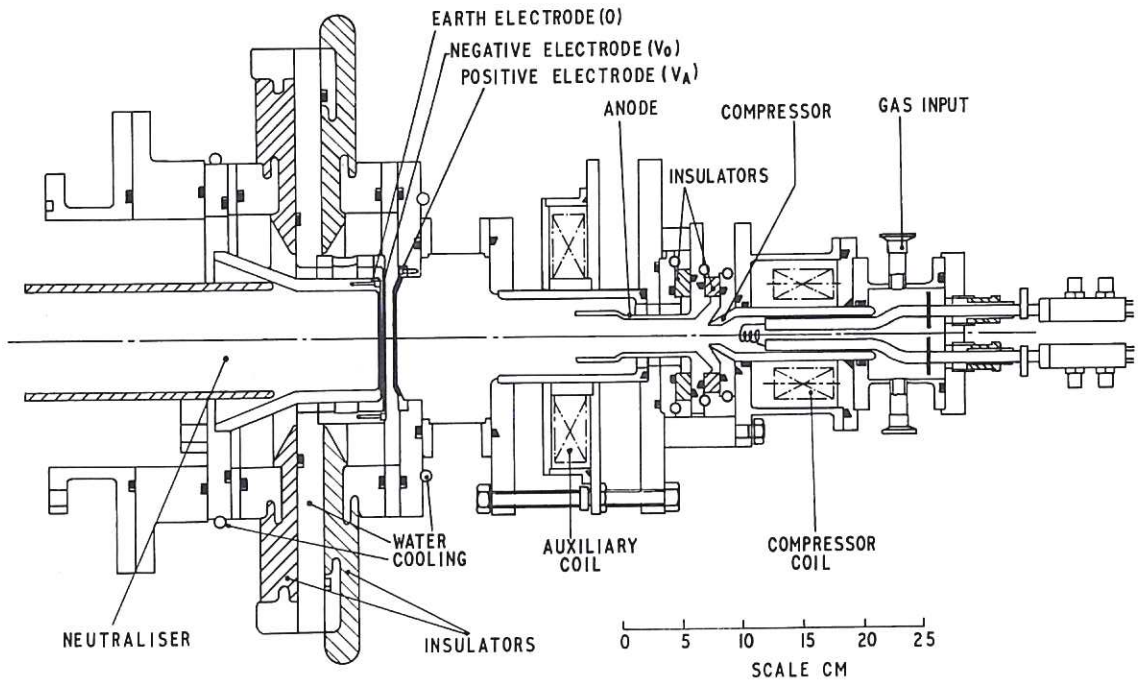


Fig. 7 The Mk II multiaperture source

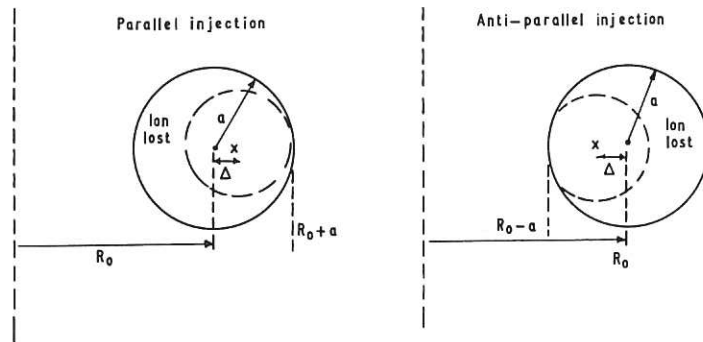


Fig. 8 Ion containment and loss regions for parallel and anti-parallel injection

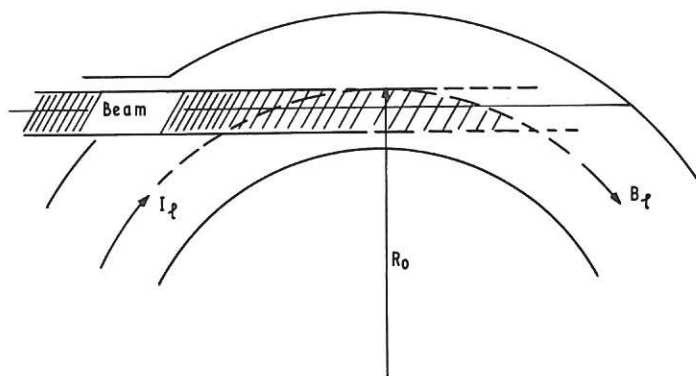


Fig. 9 The neutral beam path for the first injection system

